

Article

Structural and Electrical Parameters of ZnO Thin Films Grown by ALD with either Water or Ozone as Oxygen Precursors

Aleksandra Seweryn ^{*}, Rafal Pietruszka , Bartłomiej S. Witkowski, Aleksandra Wierzbicka, Rafal Jakiela, Piotr Sybilski and Marek Godlewski

Institute of Physics, Polish Academy of Sciences, Aleja Lotnikow 32/46, PL-02668 Warsaw, Poland; pietruszka@ifpan.edu.pl (R.P.); bwitkow@ifpan.edu.pl (B.S.W.); wierzbicka@ifpan.edu.pl (A.W.); jakiela@ifpan.edu.pl (R.J.); piotr.sybilski@ifpan.edu.pl (P.S.); godlew@ifpan.edu.pl (M.G.)

* Correspondence: aseweryn@ifpan.edu.pl

Received: 30 August 2019; Accepted: 22 October 2019; Published: 24 October 2019



Abstract: Low temperature (at 100 °C and below) growth of ZnO thin films by atomic layer deposition (ALD) is demonstrated. Properties of the layers grown with two different oxygen reagents: ozone and water are compared. Diethylzinc (DEZ) was used as metal precursor. Electrical and structural properties of films obtained at several different growth temperatures, ranging from 50 °C to 250 °C were analyzed. It turned out that the film grown in the water-based process at 250 °C and all films grown with ozone have more ordered crystallographic structure with the privileged growth direction (001) perpendicular to the substrate than water-based samples grown in temperatures 100–200 °C. Higher free electron concentration at room temperature was observed for ozone-based samples grown at 100 °C and 150 °C in comparison to water-based samples obtained at the same growth temperature. Low value of resistivity in case of ozone-based samples grown at 100 °C is a promising result, however lower electron mobility requires further optimization.

Keywords: zinc oxide; TCO films; thin layer

1. Introduction

In₂O₃:Sn (ITO), widely used as a transparent electrode has become too expensive due to increasing costs of indium. Thus, alternative transparent conductive oxide (TCO) materials are intensively studied for this application. The list of investigated materials is long (including, e.g., SnO₂, SnO₂:Sb, SnO₂:F, ZnO, ZnO:Al (AZO), ZnO:Ga (GZO), ZnO:F (FZO), CdO, Cd₂SnO₄, CdSnO₃, CdIn₂O₄, Zn₂SnO₄, MgIn₂O₄, CdSb₂O₆, and In₄Sn₃O₁₂ [1–7]). In most of the cases reported electrical (resistivity) and optical (transparency) properties of these materials are good enough for their use as TCO films [8–12], with ZnO-based layers considered as the most likely replacement of ITO [9–12]. This is not only due to good electrical and optical parameters of ZnO-based TCO films, but also to low costs of this material.

ZnO can be deposited by several methods [8–12], including VAPE (vacuum arc plasma evaporation) [8], MOMBD (metal organic molecular beam deposition) [9], MOCVD (metal organic chemical vapor deposition) [10], sputtering [11], PLD (pulsed laser deposition) [12], or ALD (atomic layer deposition) [13,14]. Recent investigations demonstrated that the ALD technology is one of the most prospective deposition methods of ZnO-based TCO films [13,14]. ALD is a highly flexible growth method allowing uniform coating of large substrates and multi-substrate processes. For ZnO deposition by ALD both inorganic [14,15] and organic [14,16–19] zinc precursors are possible. In the latter case the best results were achieved with dimethylzinc (DMZ, Zn(CH₃)₂) and diethylzinc (DEZ, Zn(C₂H₅)₂), using water as an oxygen precursor [16,17]. The parameters of ALD grown ZnO layers

reported by our group, i.e., free electron concentration in the range of 10^{20} cm^{-3} , resistivity in the range of 10^{-3} to $10^{-4} \Omega\text{cm}$, and transparency between 80% and 90%, are sufficient for TCO applications [20], as verified by us in various test devices [21,22]. For example, ZnO films were used as transparent electrodes in GaN-based structures [21], electrodes in Si-based photovoltaic (PV) devices [22], and inorganic elements in hybrid diodes [14,18]. The parameters given above were achieved in films deposited at relatively low temperatures (in the range of 150–200 °C) or in intentionally doped samples. However, this deposition temperature is still too high for some applications, which was the motivation for the present work.

An advantageous property of the ALD process is the relatively low deposition temperature. Our group reported that high quality ZnO films can be deposited at temperatures below 200 °C [16,17]. Nevertheless, as already stated above, for some applications a lower deposition temperature will be advantageous. For example, conventional Si-based photovoltaics can soon be replaced by the one based on organic films [23,24]

To improve the time stability of such devices, the deposition temperature of the top transparent electrode should be reduced. In the present work we consider such a possibility by testing two ALD procedures. The properties of ZnO films deposited with either water or ozone as oxygen precursor are compared to verify the feasibility of low temperature ALD processes.

This attempt was undertaken in spite of earlier reports stating that ozone-based ALD processes require higher deposition temperatures [14,25–35]. Properties of ZnO films deposited by ALD with either water or ozone as an oxidant were already compared in Ref. [32]. However, while the water-based ALD films were grown at a wide range of temperatures, starting from 120 °C, the ozone-based ALD films were deposited at higher temperatures, from 230 to 300 °C. The data on growth conditions were quite confusing or even contradicting. It was even claimed that ZnO cannot be grown using ozone at low temperature. Apparently, due to modified surface reactions a higher growth temperature is required [32]. Surprisingly long pulse times were also claimed [35]. These limitations on growth conditions are, however, not confirmed by the present data.

2. Materials and Methods

2.1. Substrate Preparation

The zinc oxide layers were deposited on $1 \times 1 \text{ cm}^2$ quartz plates (for optical and electrical examinations in particular) and on high resistivity silicon (100). The substrates were washed before mounting in the growth chamber. This was done to eliminate any contaminants that may affect the adhesion of the ZnO films to the substrate and thus ensure the homogeneity of the deposited layers. The washing process in the ultrasound cleaner (bath temperature 37 °C) was repeated three times for 5 minutes: once in isopropanol and twice in deionized water. Subsequently, the substrates were thoroughly dried in nitrogen purge of 5.0 purity.

The prepared substrates were placed in the reactor growth chamber. Prior to the process, the reactor chamber was preheated to a predetermined growth temperature. The process was carried out under vacuum below 0.5 Torr. In the case of ozone-based ALD processes, before each deposition process the test procedure of the ozone generator was run according to manufacturer's recommendations.

2.2. ALD Technology

The growth of the films was carried out in the Savannah-100 Cambridge NanoTech (now Veeco) reactor using nitrogen of 6.0 purity as the purging gas. We used an organic metal precursor: diethylzinc (DEZ, $\text{Zn}(\text{C}_2\text{H}_5)_2$, CAS number 557-20-0), and as an oxygen precursor either deionized water or ozone. Ozone was generated from the Savannah Ozone Generator with access to oxygen of purity 5.0. The maximum capacity of the ozone generator was $\sim 120 \text{ mg/L}$ ($\sim 7.5 \text{ wt.}\% \text{ O}_3$). First, we performed the test processes to establish the growth rate at given times of precursor pulses at different growth temperatures (T_g) for ozone-based processes. We tested several pulse times for both ozone and DEZ at

various growth temperatures. Surprisingly, quite short pulse times turned out to be possible, even 100 times shorter than the ones reported in Ref. [35]. The pulse length is thus close to the ones used in Ref. 34. Finally, we selected 20 ms for ozone, since for longer pulses (up to 50 ms) similar growth rates (0.73 Å/cycle and 0.72 Å/cycle, respectively) were found and lack of uniformity was observed. For DEZ we increased the pulse time to 60 ms, since for shorter ones non-uniform deposition was also observed. In the case of water-based ALD processes we used procedures optimized previously [16,17]. The same zinc conditions for water-based processes as in case of ozone-based, were giving similar results. Therefore, the zinc pulse length was 60 ms in all cases. Purge times 4s and 8s were tested, no effect on the growth rate was observed. Thus, 4 s for ozone-based processes was selected. Then we carried out the deposition processes using the above optimized growth parameters. The number of cycles was chosen to obtain layers of similar thicknesses (d, about 100 nm) for each growth temperature and oxygen precursor. This was based on our previous observation that resistivity of the films depends on their thickness [16,17]. To verify the optimized growth conditions we tested the resulting coatings for their structural, electrical, and optical properties.

2.3. Measurements Equipment

A NanoCalc 2000-UV/VIS (Micropack GmbH, Ostfildern, Germany) system with specific software (Micropack GmbH, Nanocalc 2.3.3, Ostfildern, Germany) was applied to measure the thickness of the layers. Top-view and cross section images (to verify film thickness) of the coatings were taken by scanning electron microscopy (SEM) with 1,5 nm resolution, using a Hitachi SU70 spectrometer (Hitachi Ltd. Tokyo, Japan). A secondary electron detector was used, and images were collected at 15 kV electron accelerating voltage. The crystallinity and phase composition of the layers were determined by X-ray diffraction (XRD) investigations. A Panalytical X'Pert Pro MRD diffractometer (Panalytical, Almelo, Netherlands) was used, equipped with: A X-ray tube generating radiation at a wavelength of 1.54056 Å, a hybrid two-bounce Ge (220) monochromator, and a Pixel detector [36]. Measurements were performed in two diffraction modes: in coplanar and non-coplanar Grazing Incidence X-ray diffraction (GIXRD) geometries [37,38]. The $\theta/2\theta$ XRD scans in the first geometry allowed us to determine lattice parameters, the FWHM of diffracted peaks, as well as identify the phase and orientation. The second geometry was used to separate the XRD signal coming from the Si substrate and to determine precisely the phase and orientation of the crystallites [38]. The incident X-ray beam angle was equal to 1°, which allowed us to detect diffraction peaks stemming only from the ZnO layer. Electrical parameters were obtained from Hall effect measurements. A RH2035 Phys-Tech GmbH system operating at a magnetic field of $B = 0.426$ T was used. The measurements were carried out at room temperature in the Van der Pauw mode. Electrical contacts (Al) were sputtered by a PVD 75 Kurt J. Lesker system. The content of non-intentional dopants was determined with use of secondary ion mass spectroscopy (SIMS) in a CAMECA IMS6F system. SIMS measurements were performed with a cesium (Cs⁺) primary beam, at an energy of 14,5 keV with the current kept at 50 nA. The size of the raster was about 150 × 150 microns and the secondary ions were collected from a central region of 60 microns in diameter. Secondary ions H⁻, NO⁻, C⁻, Si⁻ and ZnO⁻ as reference signal were collected. Transmission spectra were measured in the wavelength range from 300 to 800 nm at room temperature using a Varian-Cary5000 spectrophotometer.

3. Results

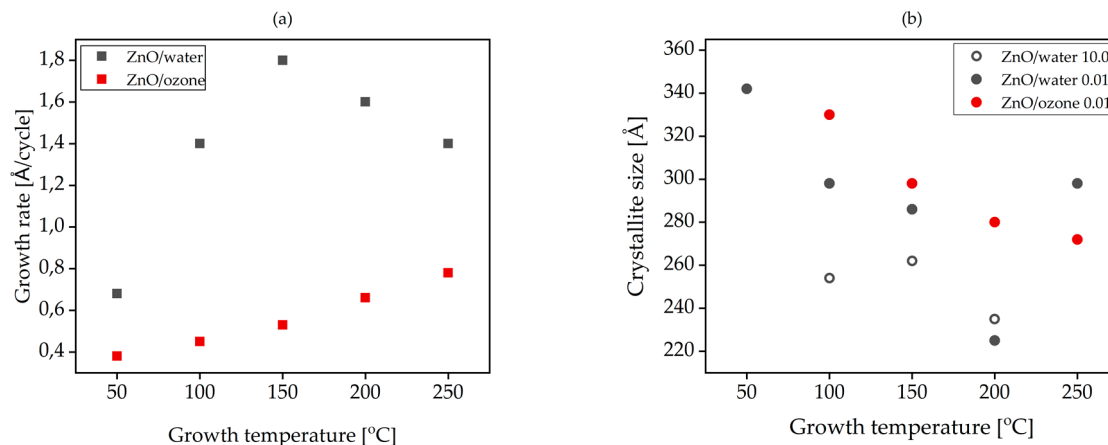
Details on the growth parameters for both types of ALD processes are given in Table 1.

Table 1. Parameters of atomic layer deposition (ALD) processes applied to obtain ZnO layers with use of diethylzinc (DEZ) and either water or ozone as precursors.

DEZ Pulse [s]	Purge [s]	Water/Ozone Pulse [s]	Purge [s]	T_g [°C]	Water-Based		Ozone-Based	
					d [nm]	Growth Rate [Å/cycle]	d [nm]	Growth Rate [Å/cycle]
0.06	4	0.02	4	50	104	0.7	107	0.4
0.06	4	0.02	4	100	100	1.4	100	0.5
0.06	4	0.02	4	150	98	1.8	102	0.5
0.06	4	0.02	4	200	99	1.6	104	0.7
0.06	4	0.02	4	250	102	1.4	104	0.8

The observed growth rates of ZnO deposited with the use of ozone was considerably lower than that in the case of water-based ALD (ZnO/water) processes. This is in line with previous observations [14,32]. However, despite the earlier report claiming that deposition temperatures exceeding 200 °C are required [32]), ZnO films can be grown even at 50 °C, making the ozone-based ALD process highly attractive. Even though much shorter DEZ and ozone pulses were applied than in Refs. [32] and [35] (both were in the range of ms instead of seconds) the resulting growth rate is quite similar to the ones reported in Reference [32]. The growth rate for the ozone-based processes increases with growth temperature, but it is still lower than that for the water-based process, contrary to the results given in Reference [32]. At temperatures above 150 °C the growth rate for the water-based processes slightly decreases.

The relevant data on the growth rate are shown in Figure 1a. We used these data to estimate the required number of ALD cycles to obtain ZnO films with comparable thicknesses for the water-based and the ozone-based ALD processes.

**Figure 1.** (a) Growth rate of ZnO layers vs. growth temperature for water-based and ozone-based processes. (b) Crystallite size in the obtained layers depending on crystallographic orientation: (10.0) and (00.1).

Figures 2 and 3 show SEM images (top views and cross-sections) of ALD films grown on silicon at five different growth temperatures with use of ozone and water as oxygen precursors, respectively. Significant differences are observed for the two types of the ALD processes in the top-view images. For both types of precursors a columnar growth was observed, which is typical for ZnO grown by ALD [16,17]. Columnar growth and column orientation in both types of ALD processes are better seen in the cross-section images, also shown in Figures 2 and 3. In the case of water-based processes the columns are disordered (i.e., not well oriented), while the ozone-based samples exhibit more

ordered columns (oriented along the growth direction) for growth temperatures of 100 °C and above. The ozone-based ZnO film grown at the lowest temperature (50 °C) is amorphous.

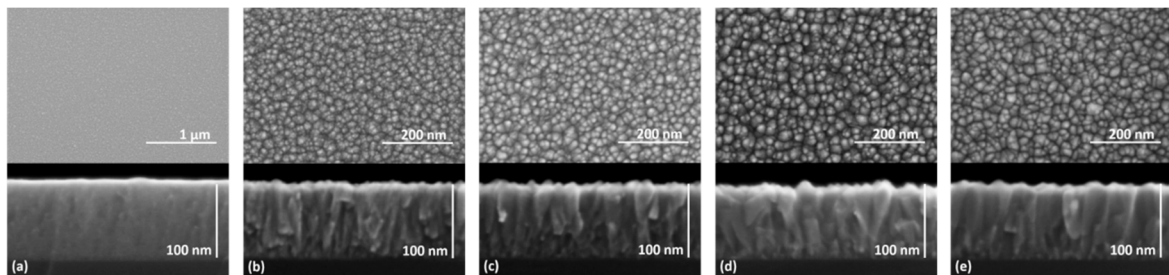


Figure 2. SEM images of analyzed ZnO ozone-based samples: top-view (**top panel**) and cross section (**bottom panel**). The results for samples grown at 50 °C (**a**), 100 °C (**b**), 150 °C (**c**), 200 °C (**d**), and 250 °C (**e**) are shown.

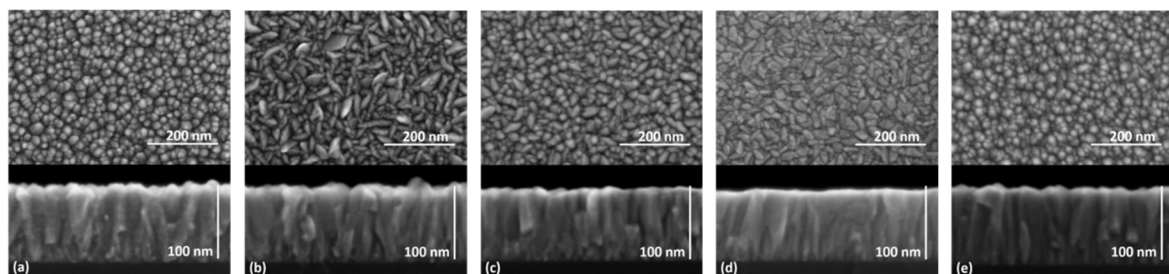


Figure 3. SEM images of analyzed ZnO water-based samples: top-view (**top panel**) and cross section (**bottom panel**). The results for samples grown at 50 °C (**a**), 100 °C (**b**), 150 °C (**c**), 200 °C (**d**), and 250 °C (**e**) are shown.

SEM results are supported by XRD examinations. First X-ray diffraction $\theta/2\theta$ scans were measured in a wide-angle range. The observed broadening of the relevant XRD peaks allowed us to estimate the column diameters with use of the Scherrer formula (Figure 1b). For the less well oriented water-based films the average column size was determined for both observed alignments, i.e., perpendicular and parallel to the growth direction. Figure 4 shows the results of non-coplanar GIXRD measurement for the water-based (Figure 4a) and ozone-based samples (Figure 4b). Only the wurtzite phase of ZnO is observed in the layers. As can be seen in all the ozone-based samples as well as in the water-based ZnO layer obtained at 250 °C the 00.2 XRD reflection is dominant. In other water-based ZnO layers more crystallographic orientations are registered.

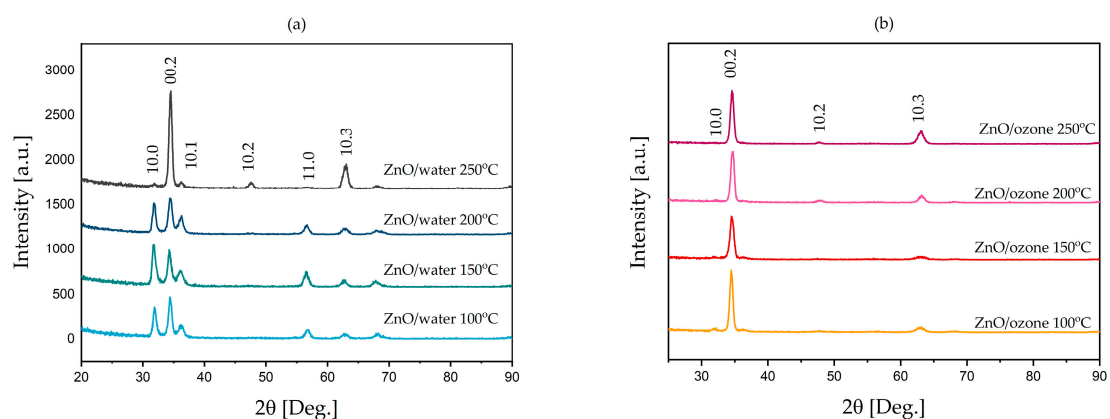


Figure 4. Non-coplanar grazing incidence X-ray diffraction (GIXRD) data of the measured layers: (a) ZnO water-based samples (b) and ZnO ozone-based samples.

Despite different growth rates the average diameters of columns aligned in the growth direction are similar for both types of ALD samples, as shown in Figure 1b. However, columns parallel to the substrate (in water-based samples) are noticeably narrower.

SIMS investigations were performed to determine the concentration of unintentional impurities in the films (see Figure 5). Carbon and hydrogen concentrations are the highest in both types of samples deposited at 50 °C. This may be due to high concentration of precursors and reactions taking place during the growth process at the lowest temperature. The impurity concentrations drop rapidly with increasing growth temperature and become comparable in water- and ozone-based layers grown at 200 °C and 250 °C.

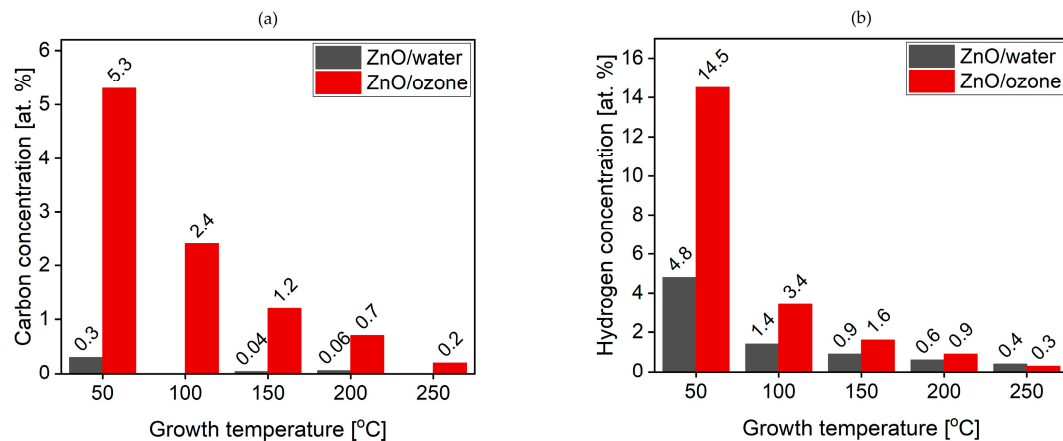


Figure 5. Secondary ion mass spectrometry (SIMS) data show concentration of unintentional dopants: (a) carbon and (b) hydrogen in ZnO ozone-based and water-based ALD samples.

In Table 2 we present electrical parameters for all the samples grown above 50 °C. The layers grown at 50 °C with ozone or water were highly resistive. The carrier concentrations in the ozone-based samples grown at 100 °C and 150 °C are significantly higher than in the water-based samples for corresponding growth temperatures. The carrier mobility is consistently higher in the water-based samples than in ozone-based samples. Table 3 shows the electrical parameters for all the samples after five minutes annealing in argon gas.

Table 2. Electrical parameters of investigated ZnO water-based and ZnO ozone-based samples: resistivity (ρ), carrier concentration (n), carrier mobility (μ).

T_g [°C]	ρ [$\Omega\cdot\text{cm}$]		n [cm^{-3}]		μ [$\text{cm}^2/\text{V}\cdot\text{s}$]	
	ZnO/O ₃	ZnO/H ₂ O	ZnO/O ₃	ZnO/H ₂ O	ZnO/O ₃	ZnO/H ₂ O
100	1.9	15	1.5×10^{19}	1.4×10^{17}	0.4	3
150	1.7×10^{-1}	6.9×10^{-2}	5.5×10^{19}	7.5×10^{18}	1	12
200	6.4×10^{-2}	6.6×10^{-3}	1.6×10^{19}	3.4×10^{19}	6	27
250	1.2×10^{-2}	9.6×10^{-3}	2.9×10^{19}	2.3×10^{19}	17	28

Table 3. Electrical parameters of investigated ZnO water-based and ozone-based samples: resistivity (ρ), carrier concentration (n), carrier mobility (μ); after post-growth annealing in argon (5 min, 500 °C).

T_g [°C]	ρ [$\Omega\cdot\text{cm}$]		n [cm^{-3}]		μ [$\text{cm}^2/\text{V}\cdot\text{s}$]	
	ZnO/O ₃	ZnO/H ₂ O	ZnO/O ₃	ZnO/H ₂ O	ZnO/O ₃	ZnO/H ₂ O
100	9.4×10^{-2}	2.5×10^{-2}	2.2×10^{19}	1×10^{17}	13	24
150	1.8×10^{-2}	2.2×10^{-2}	4.6×10^{19}	1×10^{18}	7.4	27
200	1×10^{-1}	2.9×10^{-2}	8.5×10^{19}	9.7×10^{19}	7.1	22
250	1.3×10^{-2}	1.9×10^{-1}	3.7×10^{19}	4.9×10^{19}	13	6.8

Figure 6a,b shows the optical transmission spectra for two types of the ZnO films. Due to higher electron concentration in the ozone-based films the absorption edge is surprisingly shifted to shorter wavelengths, which may be due to the Burstein-Moss effect. This is only a tentative explanation. The role of the Burstein - Moss effect can only be verified for water-based samples grown at low temperatures using the approach described in reference [39]. For ozone-based samples the data were too scattered to verify this statement.

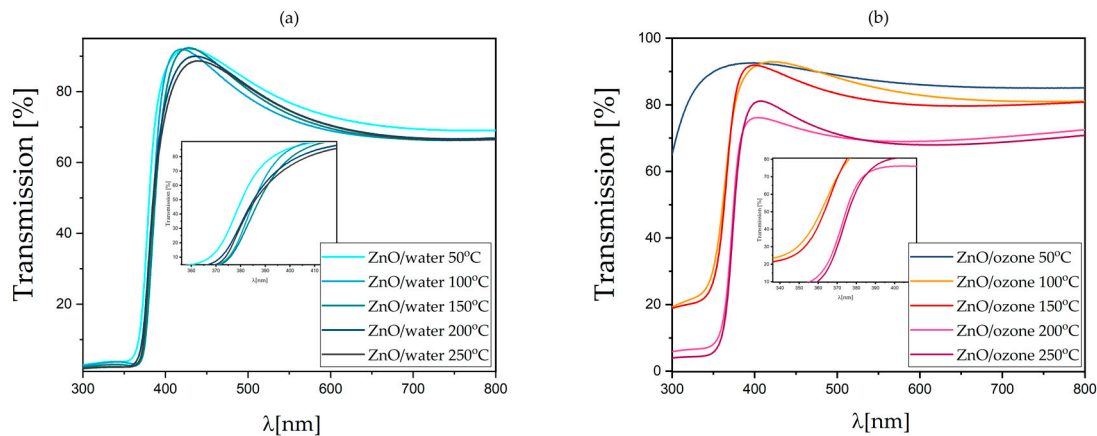


Figure 6. The data of optical transmission spectra for two types of the ZnO samples: the water-based samples (a) and the ozone-based samples (b). Insets shows enlarged displacement of relevant lines.

The transparency of the films is in the range of 80% for spectra not calibrated for quartz transmission. After calibration the transmission approaches 90%, i.e., it is better than required for the TCO films. Concluding, optical parameters of both types of films are sufficient for the intended applications.

4. Discussion

Several oxygen precursors were tested for ZnO deposition by the ALD technology [14]. Among them ozone was considered as a potentially attractive oxygen precursor not only for ZnO but also for many other oxides [25–31]. The possibility of low temperature deposition was underlined in the case of Y_2O_3 growth [31]. However, for ZnO, it was concluded that the use of O_2 , O_3 , and N_2O instead of water allows similar growth rates to those achieved in water-based processes, but only at higher deposition temperatures [14]. The available published data on the ozone-based growth processes of ZnO seem to confirm this conclusion [32–35]. ZnO ozone-based films were deposited at temperatures above 200 °C [32–35]. Moreover, the low temperature deposition was claimed to be impossible [32]. Surface etching by ozone was reported [40], questioning the use of ozone in the ALD processes of ZnO. Another mechanism which can account for a low growth rate is the ozone absorption at the ZnO surface [34]. Ozone absorption at ZnO surface may reduce the surface concentration of hydroxyl groups (OH), which are important to initiate the ALD process. It was also proposed that ozone may react with hydrocarbon groups in the DEZ precursor forming CO_2 and H_2O . The water produced in this reaction will react with DEZ leading to ZnO deposition [32]. Such possibilities require further investigations. We can only conclude that the mechanism of growth is still not clear. We could not verify whether the model analyzed in Ref. 35 accounts for our data.

The present data indicate, however, that low temperature deposition of ZnO is possible and that ZnO/ozone films have quite attractive properties. As shown in Table 2, up to two orders of magnitude higher electron concentrations can be achieved by replacing water pulses with the ozone ones. Only for deposition temperatures in the range of 200–250 °C the electron concentration for the two types of ALD processes tested by us becomes comparable. These data should be compared with the ones given Ref. [32]. Whereas the higher resistivity of ozone-based films agrees with the previous observation [32], data on carrier mobility and concentration differ. In both types of samples,

the electron mobility and concentration increase with increasing deposition temperature. This agrees with our previous observation for water-based samples [16,17]. The present data do not support the proposition given in Ref. 32. It was proposed that the higher resistivity of ozone-based films may be due to silicon contamination of samples deposited on Si substrates. To verify such a possibility electrical measurements were performed for samples deposited on quartz. These data are given in Tables 2 and 3. A significantly higher resistivity of ozone-grown films is also observed in the case of films grown on quartz substrates. Moreover, SIMS data do not confirm high Si concentration in the samples grown on silicon.

Hydrogen concentration was of interest to explain increased free electron concentration (see Table 2) observed in ozone-based ALD ZnO samples. We also wanted to verify previous suggestion that the layer crystallization may depend on defects/dopants concentration in the films (influence of carbon was suggested in [14,41]). In fact, high carbon concentration detected in ZnO/ozone films grown at 50 °C may be responsible for the suppression of crystallization of these films, since such films are amorphous. This assertion requires, however, further investigations. Carbon concentration is still high in films grown at 100 °C but they are already crystalline. Moreover, optical transmission data suggest that samples grown at 50 °C contain different compounds.

SIMS investigations (see Figure 5b) show much higher hydrogen concentrations in ZnO/ozone films deposited at extremely low temperatures from 100 °C to 150 °C. This might be the reason for the higher free electron concentration in ozone-based films. Hydrogen is considered as a shallow donor dopant in ZnO [42,43]. However, present data do not support this explanation. With increasing deposition temperature both hydrogen and carbon concentrations drop rapidly, whereas the free electron concentration either is only weakly affected (in ozone-based samples) or even rises (in water-based processes). This questions the role of hydrogen as the dominant shallow donor in our ZnO films, in particular those obtained at higher temperatures (200 °C and 250 °C). In previous investigations it was suggested that interstitial zinc can be the dominant shallow donor in ALD-deposited ZnO [16,17]. This was proposed for films grown with water as oxidant. Interstitial zinc may possibly occur also in ozone-based samples.

Despite the higher free electron concentration, the observed resistivity of ozone-based ZnO films is higher than that of films grown with water as oxygen precursor. The data presented in Table 2 indicate consistently lower carrier mobility in the ozone-based samples. This reduces the sample conductivity and thus increases the resistivity. A similar situation was also reported in Ref. 32. The resistivity in ZnO/ozone samples is too high for TCO applications.

The lower mobility may be due to the better column alignment in the ZnO/ozone films and/or a higher defect concentration in such films. SEM and XRD investigations indicate that films grown with water are less ordered, with many columns aligned perpendicular to the growth direction, i.e., along the current flow. Considering the expected inhomogeneous character of carrier scattering (the dominant mechanism being due to scattering at grain/column boundaries [44]), more efficient scattering is expected in the films with columns aligned along the growth direction. Such situation may occur in the films grown with ozone. The data presented in Figure 1b show that the average sizes of grains/columns in both types of the films are quite comparable and depend only weakly on the deposition temperature. Thus, not column diameters but their orientation seems to be more important.

However, we cannot reject an alternative explanation. Lower electron mobility in the ZnO/ozone samples can relate to a higher defect concentration in such films. To check this, we annealed the films in argon, first at 100 °C and subsequently at 500 °C (for five minutes). Then we measured the electrical properties of the annealed samples. The lower annealing temperature had practically no effect on the sample properties. For the higher annealing temperature, we observed a significant change of carrier mobility (see Table 2). The effect of annealing at this condition requires further investigations. In our previous studies [16,17] we observed that annealing at temperatures about 500 °C and higher introduces some defects, such as vacancies, which affect the electrical parameters of samples. After post-growth annealing the electron mobility of the sample grown with ozone at 100 °C increased by a

factor of 8, whereas the electron concentration was nearly the same. However, the electron mobility in this sample was still lower than that in the ZnO/water samples. In the latter the mobility also increased after post-growth annealing, but only in the case of samples grown below 200 °C.

These results are still not conclusive. However, we believe that the first explanation (column orientation) is more likely to account for the observed differences in electrical properties of the films grown at the lowest temperature. This statement seems to be supported by the observed decreasing difference in electron mobility of ZnO/ozone and ZnO/water films grown at 200 °C and 250 °C. While in layers grown at 100 °C the mobility in the ZnO/ozone film is nearly 10 times lower than in the ZnO/water layer, it is quite comparable for higher growth temperatures (17 cm²/Vs and 28 cm²/Vs, respectively).

The data shown in Figure 1b may partly explain the spread of information on ozone based ALD processes. The growth rate for ALD processes with use of water is higher. This is in agreement with the general conclusion given in Ref. 14. Several mechanisms were proposed to explain why ozone-based processes require higher growth temperatures and why growth rates are lower. For example, in Reference 40 etching of the surface layer by ozone was claimed. Ozone reaction with DEZ or ozone absorption on the surface [32,34,35] were also proposed. Despite these suggestions the present data prove that ultra-low temperature ALD processes with ozone as oxidant are possible, resulting in ordered films with a high electron concentration at room temperature. For some applications (e.g., in hybrid structures) this is an important conclusion. For TCO applications further process optimization is necessary to reduce the resistivity of ozone-based films, whereas optical parameters are already as required.

5. Conclusions

The present data indicate attractive properties of ZnO films grown with ozone as oxidant. High quality films can be deposited at very low growth temperature. This is important as tested by us feasibility of the ALD deposition method for applications in organic-based electronics, optoelectronics, and photovoltaics. The obtained films show high transparency, but still too high resistivity. However, further optimization of ozone-based processes is possible.

Author Contributions: Conceptualization, M.G. and A.S.; methodology, R.P. and A.S.; validation, A.S. and M.G.; formal analysis, A.S., R.J. and R.P.; investigation, A.S., R.P., B.S.W., R.J., A.W., P.S.; resources A.S. and R.P.; writing—original draft preparation, M.G. and A.S. and A.W.; writing—review and editing M.G. and A.S.; visualization, A.S. supervision, M.G.; project administration, M.G.; funding acquisition, M.G.

Funding: This work was partially supported by the National Centre for Research and Development TECHMATSTRATEG1/347012/NCBR/2017, TECHMATSTRATEG1/347431/14/NCBR/2018.

Acknowledgments: The authors thanks dr. hab. Hanka Przybylińska, prof. IP PAS for helpful discussions.

Conflicts of Interest: The authors declare no conflict of interest.

References

1. Dawar, A.L.; Joshi, J.C. Semiconducting transparent thin films: their properties and applications. *J. Mater. Sci.* **1984**, *19*, 1. [[CrossRef](#)]
2. Chopra, K.L.; Major, S.; Pandya, D.K. Transparent Conductors—A Status Review. *Thin Solid Films* **1983**, *102*, 1. [[CrossRef](#)]
3. Hartnagel, H.L.; Dawar, A.L.; Jain, A.K.; Jagadish, C. *Semiconducting Transparent Thin Films*, 1st ed.; Institute of Physics Publishing: Bristol, UK; Philadelphia, PA, USA, 1995.
4. Enoki, H.; Nakayama, T.; Echigoya, J. The Electrical and Optical Properties of the ZnO-SnO₂ Thin Films Prepared by RF Magnetron Sputtering. *Phys. Status Solidi.* **1992**, *129*, 181. [[CrossRef](#)]
5. Un'no, H.; Hikuma, N.; Omata, T.; Ueda, N.; Hashimoto, T.; Kawazoe, H. Preparation of MgIn₂O_{4-x} Thin Films on Glass Substrate by RF Sputtering. *Jpn. J. Appl. Phys.* **1993**, *32*, L1260. [[CrossRef](#)]
6. Yanagawa, K.; Ohki, Y.; Omata, T.; Hosono, H.N.; Ueda, N.; Kawazoe, H. Preparation of Cd_{1-x}Y_xSb₂O₆ thin film on glass substrate by radio frequency sputtering. *Appl. Phys. Lett.* **1994**, *65*, 406. [[CrossRef](#)]

7. Minami, T.; Takeda, Y.; Takata, S.; Kakumu, T. Preparation of transparent conducting In₄Sn₃O₁₂ thin films by DC magnetron sputtering. *Thin Solid Film*. **1997**, *13*, 308–309. [[CrossRef](#)]
8. Uramoto, J. An Ion Source Plasma starting from a cold LaB₆ cathode I. *Res. Rep. Inst. Plasma Phys.* **1979**, *1*, 25.
9. Sato, H.; Minami, T.; Takata, S.; Miyata, T.; Ishii, M. Low temperature preparation of transparent conducting ZnO:Al thin films by chemical beam deposition. *Thin Solid Film*. **1993**, *236*, 14. [[CrossRef](#)]
10. Gordon, R.G. Criteria for Choosing Transparent Conductors. *MRS Bull.* **2000**, *25*, 52. [[CrossRef](#)]
11. Minami, T.; Sato, H.; Nanto, H.; Takata, S. Highly conductive and transparent ZnO: Al thin films prepared on high-temperature substrates by d.c. magnetron sputtering. *Thin Solid Film*. **1989**, *176*, 277. [[CrossRef](#)]
12. Suzuki, A.; Matsushita, T.; Wada, N.; Sakamoto, Y.; Okuda, M. Surface Flatness of Transparent Conducting ZnO:Ga Thin Films Grown by Pulsed Laser Deposition. *Jpn. J. Appl. Phys.* **1996**, *35*, L56. [[CrossRef](#)]
13. Suntola, T.; Antson, J. Method for Producing Compound Thin Films. US Patent 4,058,430, 15 November 1977.
14. Tynell, T.; Karppinen, M. Atomic layer deposition of ZnO: a review. *Semicond. Sci. Technol.* **2014**, *29*, 4. [[CrossRef](#)]
15. Katsia, E.; Huby, N.; Tallarida, G.; Kutrzeba-Kotowska, B.; Perego, M.; Ferrari, S.; Krebs, F.C.; Guziewicz, E.; Godlewski, M.; Łuka, G. Poly(3-hexylthiophene)/ZnO hybrid pn junctions for microelectronics applications. *Appl. Phys. Lett.* **2009**, *94*, 143501. [[CrossRef](#)]
16. Guziewicz, E.; Kowalik, I.A.; Godlewski, M.; Kopalko, K.; Osinniy, V.; Wójcik, A.; Yatsunencko, S.; Łusakowska, E.; Paszkowicz, W. Extremely low temperature growth of ZnO by atomic layer deposition. *J. Appl. Phys.* **2008**, *103*, 033515. [[CrossRef](#)]
17. Guziewicz, E.; Godlewski, M.; Krajewski, T.; Wachnicki, Ł.; Szczepanik, A.; Kopalko, K.; Wójcik-Głodowska, A.; Przeździecka, E.; Paszkowicz, W.; Łusakowska, E.; et al. ZnO grown by atomic layer deposition: A material for transparent electronics and organic heterojunctions. *J. Appl. Phys.* **2009**, *105*, 122413. [[CrossRef](#)]
18. Stakhira, P.Y.; Pakhomov, G.L.; Cherpak, V.V.; Volynyuk, D.; Łuka, G.; Godlewski, M.; Guziewicz, E.; Hotra, Z. Photovoltaic cells based on nickel phthalocyanine and zinc oxide formed by atomic layer deposition. *Cent. Eur. J. Phys.* **2010**, *8*, 798. [[CrossRef](#)]
19. Godlewski, M.; Guziewicz, E.; Gierałtowska, S.; Łuka, G.; Krajewski, T.; Wachnicki, Ł.; Kopalko, K. Barriers in Miniaturization of Electronic Devices and the Ways to Overcome Them—from a Planar to 3D Device Architecture. *Acta Phys. Polonica A* **2009**, *116*, S19–S21. [[CrossRef](#)]
20. Godlewski, M.; Guziewicz, E.; Łuka, G.; Krajewski, T.; Łukasiewicz, M.; Wachnicki, Ł.; Wachnicka, A.; Kopalko, K.; Sarem, A.; Dalati, B. ZnO layers grown by Atomic Layer Deposition: A new material for transparent conductive oxide. *Thin Solid Films* **2009**, *518*, 1145. [[CrossRef](#)]
21. Grzanka, S.; Łuka, G.; Krajewski, T.A.; Guziewicz, E.; Jachymek, R.; Purgal, W.; Wiśniewska, R.; Sarzyńska, A.; Bering-Staniszevska, A.; Godlewski, M.; et al. Thin Film ZnO as Sublayer for Electric Contact for Bulk GaN with Low Electron Concentration. *Acta. Phys. Pol. A* **2011**, *119*, 672–674. [[CrossRef](#)]
22. Pietruszka, R.; Witkowski, B.S.; Zielony, E.; Gwozdz, K.; Placzek-Popko, E.; Godlewski, M. ZnO/Si heterojunction solar cell fabricated by atomic layer deposition and hydrothermal methods. *Solar Energy* **2017**, *155*, 1282. [[CrossRef](#)]
23. Lizin, S.; Van Passel, S.; De Schepper, E.; Maes, W.; Lutsen, L.; Manca, J.; Vanderzande, D. Life cycle analyses of organic photovoltaics: A review. *Energy Environ. Sci.* **2013**, *6*, 3136. [[CrossRef](#)]
24. Fan, Z.; Sun, K.; Wang, J. Perovskites for photovoltaics: A combined review of organic–inorganic halide perovskites. *J. Mater. Chem. A* **2015**, *3*, 18809. [[CrossRef](#)]
25. Cho, Y.J.; Chung, K.B.; Chang, H.S. Characteristics of surface passivation of ozone- and water-based Al₂O₃ films grown by atomic layer deposition for silicon solar cells. *Thin Solid Film*. **2018**, *649*, 57. [[CrossRef](#)]
26. Von Gastrow, G.; Lia, S.; Repo, P.; Bao, Y.; Putkonen, M.; Savin, H. Ozone-based batch atomic layer deposited Al₂O₃ for effective surface passivation. *Energy Procedia* **2013**, *38*, 890. [[CrossRef](#)]
27. Liu, X.; Ramanathan, S.; Longdergan, A.; Srivastava, A.; Lee, E.; Seidel, T.E.; Barton, J.T.; Pang, D. ALD of Hafnium Oxide Thin Films from Tetrakis (ethylmethylamino) Hafnium and Ozone. *J. Electrochem. Soc.* **2005**, *152*, G213. [[CrossRef](#)]
28. Kim, Y.W.; Kim, D.H. Atomic layer deposition of TiO₂ from tetrakis-dimethylamido-titanium and ozone. *Korean J. Chem. Eng.* **2012**, *29*, 969–973. [[CrossRef](#)]
29. Päiväsääri, J.; Putkonen, M.; Sajavaara, T.; Niinistö, L. Atomic layer deposition of rare earth oxides: Erbium oxide thin films from beta-diketonate and ozone precursors. *J. Alloy. Compd.* **2004**, *374*, 124. [[CrossRef](#)]

30. Martinson, A.B.F.; DeVries, M.J.; Libera, J.A.; Christensen, S.T.; Hupp, J.T.; Pellin, M.J.; Elam, J.W. Atomic layer deposition of Fe₂O₃ using ferrocene and ozone. *J. Phys. Chem. C* **2011**, *115*, 4333. [CrossRef]
31. Putkonen, M.; Sajavaara, T.; Johansson, L.S.; Niinistö, L. Low-Temperature ALE Deposition of Y₂O₃ Thin Films from β-Diketonate Precursors. *Chem. Vap. Depos.* **2001**, *7*, 44. [CrossRef]
32. Kim, S.K.; Hwang, C.S.; Park, S.H.K.; Yun, S.J. Comparison between ZnO films grown by atomic layer deposition using H₂O or O₃ as oxidant. *Thin Solid Film.* **2005**, *478*, 103.
33. Yuan, H.; Luo, B.; Campbell, S.A.; Gladfelter, W.L. Atomic Layer Deposition of p-Type Phosphorus-Doped Zinc Oxide Films Using Diethylzinc, Ozone and Trimethylphosphite. *Electrochem. Solid-State Lett.* **2011**, *14*, H181. [CrossRef]
34. Mundle, R.; Terry, H.; Bahoura, M.; Pradhan, A.K. Ozone-assisted atomic layer deposited ZnO thin films for multifunctional device applications. *J. Phys. D* **2013**, *46*, 475101. [CrossRef]
35. Warner, E.J.; Cramer, C.J.; Gladfelter, W.L. Atomic layer deposition of zinc oxide: Understanding the reactions of ozone with diethylzinc. *J. Vac. Sci. Technol. A* **2013**, *31*, 041504. [CrossRef]
36. Wierzbicka, A.; Zytkeiwicz, Z.R.; Sobanska, M.; Klosek, K.; Lusakowska, E. Influence of Substrate on Crystallographic Quality of AlGa_N/Ga_N HEMT Structures Grown by Plasma-Assisted MBE. *Acta Physica Polonica A* **2012**, *121*, 899–902. [CrossRef]
37. Colombi, P.; Zanola, P.; Bontempi, E.; Roberti, R.; Gelfib, M.; Depero, L.E. Glancing-incidence X-ray diffraction for depth profiling of polycrystalline layers. *J. Appl. Cryst.* **2006**, *39*, 177–179. [CrossRef]
38. Kobayashi, S.; Inaba, K. Introduction to XRD analysis of modern functional thin films using a 2-dimensional detector – (1) GI-XRD. *Rigaku J.* **2016**, *32*. Available online: https://www.rigaku.com/downloads/journal/RJ33-1/Rigaku%20Journal%2033-1_10-14.pdf (accessed on 22 October 2019).
39. Fujiwara, H.; Kondo, M. Effects of carrier concentration on the dielectric function of ZnO:Ga and In₂O₃:Sn studied by spectroscopic ellipsometry: Analysis of free-carrier and band-edge absorption. *Phys. Rev. B* **2005**, *71*, 075109. [CrossRef]
40. Knoops, H.C.M.; Elam, J.W.; Libera, J.A.; Kessels, W.M.M. Surface Loss in Ozone-Based Atomic Layer Deposition Processes. *Chem. Mater.* **2011**, *23*, 2381. [CrossRef]
41. Mikkulainen, V.; Leskelä, M.; Ritala, M.; Puurunen, R.L. Crystallinity of inorganic films grown by atomic layer deposition: Overview and general trends. *J. Appl. Phys.* **2013**, *113*, 021301. [CrossRef]
42. Van de Walle, C.G. Defect analysis and engineering in ZnO. *Physica B* **2001**, *899*, 308–310. [CrossRef]
43. Van de Walle, C.G. Hydrogen as a Cause of Doping in Zinc Oxide. *Phys. Rev. Lett.* **2000**, *85*, 1012. [CrossRef] [PubMed]
44. Krajewski, T.A.; Dybko, K.; Łuka, G.; Wachnicki, Ł.; Kopalko, K.; Paszkowicz, W.; Godlewski, M.; Guziewicz, E. Analysis of scattering mechanisms in zinc oxide films grown by the atomic layer deposition technique. *J. Appl. Phys.* **2015**, *118*, 035706. [CrossRef]

